DE GRUYTER
OPEN

Ion acceleration from intense laser-generated plasma: methods, diagnostics and possible applications

Lorenzo Torrisi

Abstract. Many parameters of non-equilibrium plasma generated by high intensity and fast lasers depend on the pulse intensity and the laser wavelength. In conditions favourable for the target normal sheath acceleration (TNSA) regime the ion acceleration from the rear side of the target can be enhanced by increasing the thin foil absorbance through the use of nanoparticles and nanostructures promoting the surface plasmon resonance effect. In conditions favourable for the backward plasma acceleration (BPA) regime, when thick targets are used, a special role is played by the laser focal position with respect to the target surface, a proper choice of which may result in induced self-focusing effects and non-linear acceleration enhancement. SiC detectors employed in the time-of-flight (TOF) configuration and a Thomson parabola spectrometer permit on-line diagnostics of the ion streams emitted at high kinetic energies. The target composition and geometry, apart from the laser parameters and to the irradiation conditions, allow further control of the plasma characteristics and can be varied by using advanced targets to reach the maximum ion acceleration. Measurements using advanced targets with enhanced the laser absorption effect in thin films are presented. Applications of accelerated ions in the field of ion source, hadrontherapy and nuclear physics are discussed.

Key words: ion acceleration in plasma • plasma diagnostics • TOF • target normal sheath acceleration (TNSA)

L. Torrisi
Dipartimento di Fisica e Scienze della Terra
& Dottorato di Ricerca in Fisica,
Università di Messina,
V. le F. S. D'Alcontres 31, 98166 S. Agata,
Messina, Italy,
E-mail: Lorenzo.Torrisi@unime.it

Introduction

The laser–matter interaction represents a topical subject of high interest for many aspects of the physics of non-equilibrium plasmas, plasma diagnostics and many applications in all scientific fields, ranging from physics to chemistry, from microelectronics to engineering, from medicine to biology and from cultural heritage to environmental analysis. There exists a broad literature on the possible applications of the laser-generated plasmas, such as laser ion sources [1], nuclear reactions occurring in hot plasmas [2], development of high electric fields to accelerate ions in non-equilibrium plasmas [3], multi-energetic ion implantation from plasma emission [4], the use of plasma ion acceleration in proton therapy [5], laser ablation developing plasma for archaeological and environmental applications [6].

The laser light incident on solid matter transfers high kinetic energy to electrons proportionally to the $I\lambda^2$ parameter, where I is the laser intensity (in W/cm^2) and λ (in μm) is the laser wavelength. For high laser intensities the energy transferred to electrons is related to the ponderomotive energy [7], ε_p:

$$(1) \quad \varepsilon_p = \frac{e^2 E_0^2 \lambda^2}{16\pi^2 m_e c^2} = 9.33 \times 10^{-14}(I\lambda^2) \ \ (\text{in eV})$$

where e is the electron charge, E_0 the electric field of the electromagnetic wave, m_e the electron mass and c the speed of light in vacuum. Thus, the energy transferred to electrons by a laser with 1 μm wavelength and 10^{16} W/cm^2 intensity is about 1 keV. More intense lasers produce relativistic electrons. Electron oscillations may cover distances of many lattice spacings in a solid, interacting with other atoms and inducing their ionization.

Many other plasma parameters depend on the $I\lambda^2$ factor, such as the hot electron temperature, kT_{hot}, given by the relation:

$$(2) \quad kT_{\text{hot}} = \left(\sqrt{1 + \frac{I\lambda^2}{2.8 \times 10^{18} \ \text{W}\mu^2 / \text{cm}^2}} - 1 \right) \cdot 511 \ \text{keV}$$

and corresponding to a value of about 1 keV at 1 μm wavelength and 10^{16} W/cm^2 laser intensity. As an example, the shockwave pressure, the ion temperature T_i, the emitted ion current and the electric field generated as a result of charge separation effects depend on the $I\lambda^2$ factor.

Three main regimes of high intensity laser–matter interaction can be employed. The first concerns the laser interacting with bulk targets, resulting in backward plasma acceleration (BPA), which has the advantage of producing high ion emission and high currents by using repetitive laser pulses [8]. Although ions in this regime achieve relatively low kinetic energies, generally below 1 MeV/charge state, it is of special interest in laser ion source applications and high ion emission yields. The second regime, occurring at intensities above 10^{15} W/cm^2, known as the target normal sheath acceleration (TNSA), has the advantage that it allows to accelerate ions to kinetic energies above 1 MeV/charge state [9]. In this case a high electric field is generated at the rear side of a thin irradiated target, due to relativistic electrons escaping from the target and to resulting Coulomb explosion of the target (Fig. 1b). The electric field drives the ion acceleration in forward direction along the normal to the target surface. The third regime is known as radiation pressure acceleration (RPA) regime and shows very high ion acceleration, above 10 MeV/charge state for laser intensity above 10^{19} W/cm^2 [10]. The most effective mechanism for coupling laser energy to ions is predicted to be RPA, for which the momentum of the laser is efficiently imparted to the ions. Electrons are accelerated out of the backside of the thin foil, the attractive electrostatic force between ions and electrons gives rise to a dense electron layer just behind the backside of the foil; like a sail, the dense electron layer is accelerated by the very high light pressure of the laser and the heavier ions are pulled by the dense electron layer and they are accelerated as well.

In the TNSA regime the electric field driving ion acceleration from the rear side of the target is given by the formula

$$(3) \quad E_{\text{TNSA}} = \sqrt{\frac{kT_{\text{hot}} n_e(0)}{\varepsilon_0}}$$

where $n_e(0)$ is the electron density at the target surface and ε_0 is the electric permittivity of the vacuum. Assuming a laser intensity of 10^{16} W/cm^2, 1 μm wavelength and a maximum electron density of 10^{21}/cm^3, the electric field reaches a value of 1.3×10^{11} V/m.

When thin targets are used, the ion acceleration in the forward direction is increased, but the ion yield decreases due to the low thickness, and there is increased risk that the target would become transparent to the laser light, with a consequent laser energy loss. Thus the target composition and the laser coupling to the target – in order to have high absorption of laser radiation – become an important factor of the target irradiation. To enhance the absorption properties special metallic absorbent nanostructures can be embedded in thin targets to promote the surface plasmon resonance effect at the wavelength of the laser radiation being used [11]. Plasma properties in the different regimes can be investigated using fast diagnostics, such as time-of-flight diagnostics, semiconductor detectors and a Thomson parabola spectrometer.

Experimental setup

An iodine laser operating at 1315 nm wavelength, with 300 ps pulse duration and 10^{15} W/cm^2 intensity was utilized at PALS of ASCR in Prague to generate non-equilibrium plasma and to accelerate ions. Thick and thin (less than 10 microns) targets were used to accelerate ions in BPA and TNSA regimes in high vacuum. Hydrogenated targets, based on polymers and hydrates, have been employed to produce energetic protons. Heavy metallic elements, such as gold, were employed in the form of thick or thin multilayers and nanostructures embedded in polymers in order to enhance the laser absorption in the thin targets and to induce high electric field driving the ion acceleration in forward direction.

Different diagnostics can be used to study the plasma properties and the radiation emitted from the plasma. On line diagnostics use time-of-flight (TOF) techniques to measure the ion velocity and to calculate the mean ion kinetic energy. Ion collectors and SiC detectors, connected to a fast storage oscilloscope, are employed to measure the maximum and mean ion energy: first of them give a signal proportional to the ion charge state and the second of them give a signal proportional to the ion energy deposited in the semiconductor depletion layer. Thin absorbers used in front of the detector may reduce the noise due to visible light, UV and soft X-rays detection and to stop heavy ions, permitting the detection of only protons. Ion energy analyzers (IEA), based on the electrostatic deflection of plasma emitted ions, give the ion energy distributions and charge state distributions by varying the voltage of the deflection plates. A Thomson parabola spectrometer (TPS), based on the magnetic and electric deflection of the

ions towards a multi-channel-plate (MCP) coupled to a phosphorus screen, permits to measure the mass-to-charge ratio, to identify the ion species and to measure the maximum ion energy. Streak cameras sensitive to X-rays or to visible region, for exposition times of the order of 1–2 ns, allow to obtain information about the plasma properties. Off line diagnostics use track detectors (CR-39, Gaf chromic,..), SEM microscopy, ion implanted substrates and other techniques to obtain the information on the properties of the produced plasma. In order to study the RPA regime one has to use higher intensity lasers, such as the neodymium glass Vulcan, an 8-beam 2.5 kJ per 2 ns pulse duration, at the Rutherford Appleton Laboratory's Central Laser Facility in Oxfordshire, United Kingdom. The plasma diagnostic can be optimized to detect ions with energies above 10 MeV/charge state. Vulcan laser is one of the highest intensity lasers in the world, capable of producing a petawatt laser beam with a focused intensity of 10^{21} W/cm^2.

Plasma properties and ion acceleration depend strongly on three sets of factors: the laser parameters (the pulse energy, the pulse intensity, the pulse duration,...), the irradiation conditions (the location and size of the focal point of the laser, the use of polarized light, the presence of a prepulse,...), and the target composition and geometry (the target thickness, multilayers, nanostructures, resonant absorption effects,...). Thin advanced targets are prepared at the Messina University to increase the laser energy absorption in thin foils and to decrease the reflection and transmission components so that the transfer of the laser light energy to the plasma

is maximized. In this context the optimal target thickness and the use of absorbent nanostructures embedded in the target play an important role. As an example, Fig. 1 shows the light absorption coefficient of nanostructures in the wavelength range from UV to near IR. The use of Au nanorods permits to increase the laser absorbance at specified wavelength regions, depending on their size, shape and environment. For example, high absorbance in thin targets at the PALS laser fundamental wavelength (1315 nm) can be obtained by using Au nanorods 25 nm in diameter and 240 nm in length, immersed in polymers (Fig. 1b). Nanowires, grown orthogonally to the bulk surface of AlGaAs and Si substrates, show high absorption at different wavelength bands (Fig. 1a) [12, 13], depending of their length, size and spatial nanostructure distance. The same figure shows also a scheme of the TNSA regime used for the laser ion acceleration (Fig. 1c).

Results

BPA regime

Using the BPA regime and thick targets at the PALS laboratory in Prague it is possible to accelerate ions in the backward direction to energies above 20 keV/charge state. The use of peculiar conditions of laser irradiation, such as that to induce self-focusing effects by focalising the laser in front of the target surface, permit to increase the maximum ion energy by about a factor two or three. Figure 2 shows a comparison between the IEA spectrum obtained
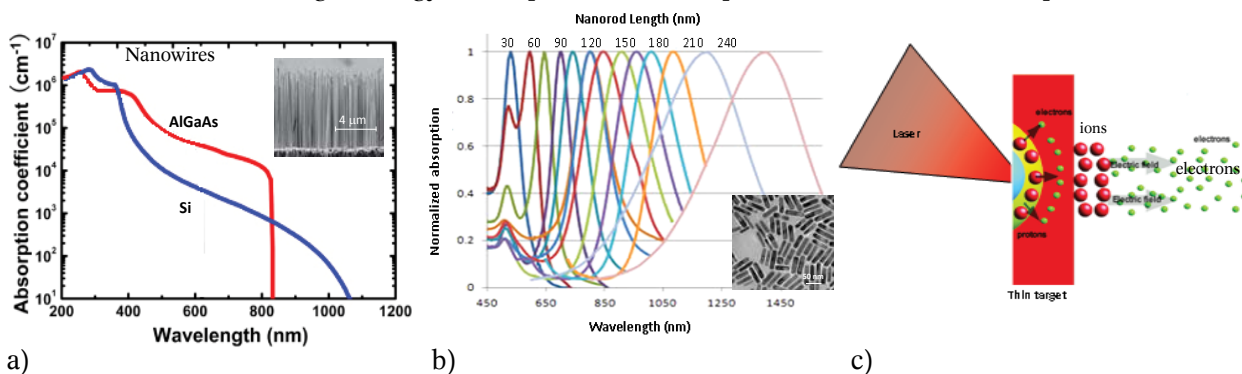

a)   b)   c)

Fig. 1. Absorption coefficient at different laser wavelengths for Si and AlGaAs nanowires (a) and Au nanorods (b), and the scheme of the TNSA regime of laser ion acceleration (c).
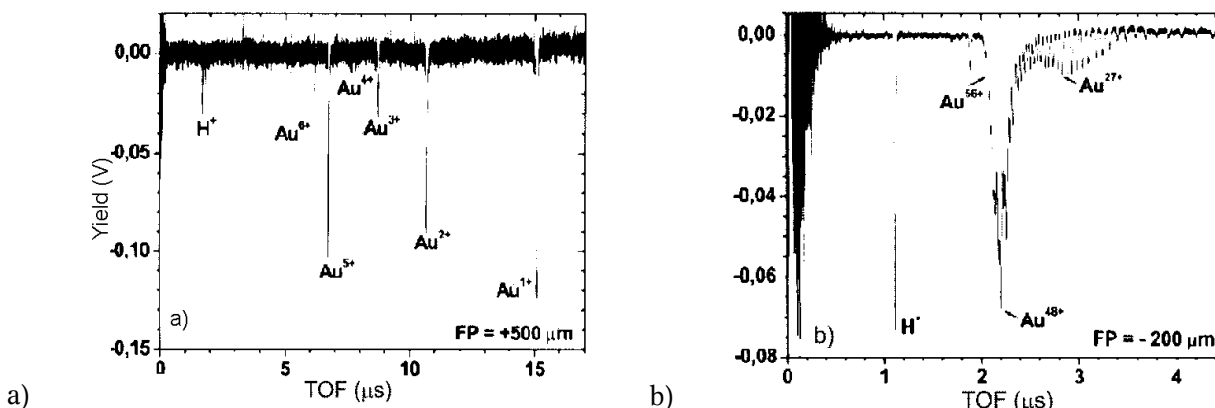

a)   b)

Fig. 2. The BPA regime of laser acceleration of Au ions without (a) and with the self-focusing effect (b).

by irradiating a thick Au target with a focal position at (a) +500 μm (focus inside the target), and (b) –200 μm (focus in front of the target) [14]. The Au charge states, from about 10+ in the first case, increase up to about 60+ in the second case. In these last conditions, in fact, a self-focusing effect occurs, the laser is further focalized by the preplasma generated on the target surface, its intensity increases and the generated plasma is hotter, producing higher charge states and more energetic ion emission. The different ion yield intensities are due to the different energy-to-charge ratio value used in the two IEA spectra acquisition systems, of about 5 keV and 10 keV per charge state in the case a) and b), respectively. It means that only one sampling of the ion Boltzmann distribution is represented in such spectra; more samplings are need to evaluate the ion energy distribution data and the ion yields versus their charge state.

TNSA regime

By using TNSA regime and thin targets at the PALS laboratory it is possible to accelerate ions in the forward direction at energies above 1 MeV/charge state. This energy can be further increased both by using self-focusing conditions and by irradiating thin advanced targets having high absorption coefficients

at the used laser wavelength. For example thin polymers containing metallic nanorods of Au can be employed in order to induce plasmon absorption resonant effect increasing the laser energy released to the plasma and enhancing the electric field driving the ion acceleration.

Figure 3 shows a typical TPS analysis of the ion emission obtained at PALS at 5×10^{15} W/cm² intensity, irradiating a 10 μm thick resin in which Au nanoparticles, 100 nm in size, are embedded at a concentration of the order of 1% in weight (a).

The parabolas analysis, performed by using a simulation program based on Opera 3D-Tosca [15], on the basis of the actual TPS geometry and of the values of the deflecting magnetic and electric fields, indicates an acceleration of about 3 MeV per charge state, so protons have a maximum energy of 3 MeV, while the Au ions, detected up to 66+ charge states, reach a maximum kinetic energy of about 200 MeV. Figure 3b shows the parabola simulation compared with the experimental data. At high laser intensity the ion kinetic energy depends mainly on the Coulomb acceleration acquired in the developed electric field and by the plasma equivalent temperature. The ion energy distributions shift towards higher energies with the increasing ion charge state and show an exponential Boltzmann-like shape with a cut-off at high energy.
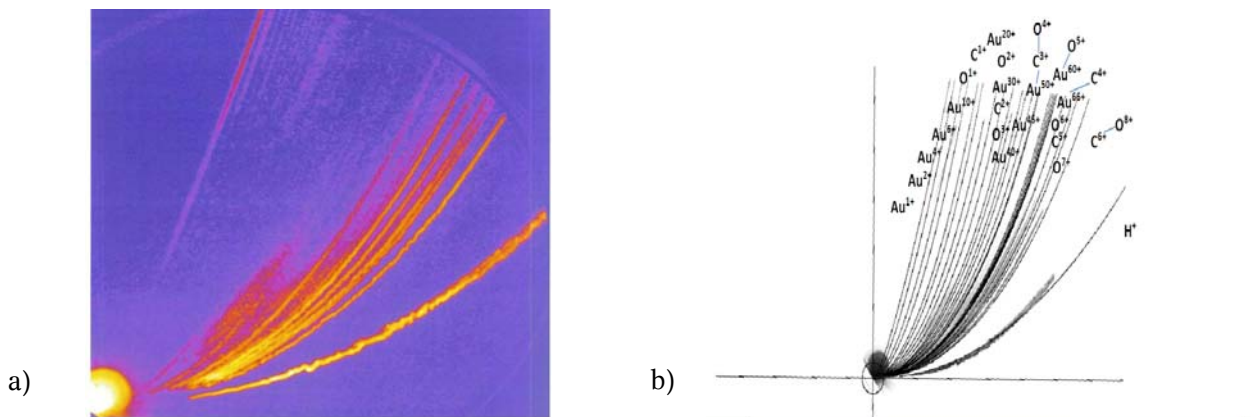

a)

b)

Fig. 3. The TPS spectrum from TNSA regime of laser acceleration ions, as obtained from MCP (a), and an image overlapping with simulation data of particle recognition (b).
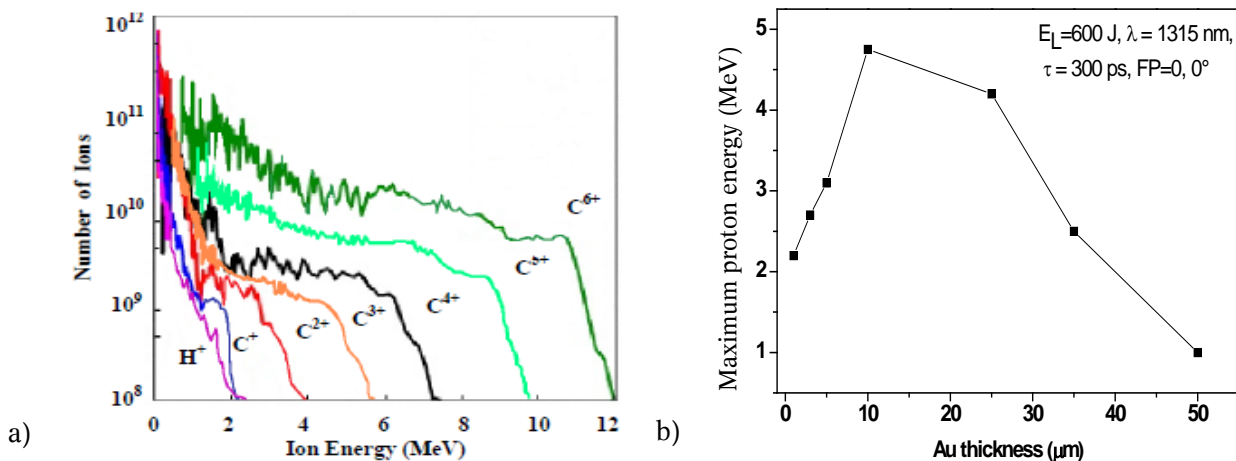

a)

b)

Fig. 4. Typical ion energy distributions obtained by irradiating a polyethylene films in the TNSA conditions at the PALS laboratory (a) and the maximum proton energy vs. Au thickness (b).

Figure 4a shows a typical example of ion energy distributions obtained by irradiating a thin foil of polyethylene – $(CH_2)_n$ is the monomer – in the TNSA conditions at the PALS laboratory. The ion acceleration in the forward direction, obtained using a 10 μm polyethylene foil, generates about 2.0 MeV/charge state, as measured by TPS and SiC. The carbon energy distributions are different for different charge states and are shifted towards high energy proportionally to their charge state. The carbon ion yields show a Boltzmann-like trend with a cut-off at the maximum ion energy. The cut-off depends on the maximum value of the generated electric field driving the ion acceleration.

The number of ions reported in the plot of Fig. 4a is relative to the yield evaluated in the forward direction within an angle of about ±30°. Due to the low thickness of the target the ion emission yield is low. Moreover the ion emission is not isotropic and the angular distribution of emitted ions is centred on the normal to the target surface with an aperture decreasing with the ion atomic mass and with the ion charge state, as reported in literature [16]. In thin films the maximum ion acceleration is obtained for an optimal thickness at which the plasma electron density has a maximum value to maximize the electric field accelerating ions. Films too thin or too thick will not generate high electron density driving the ion acceleration in the rear side of the foil. Figure 4b shows the optimal Au target thickness for proton acceleration by irradiating a thin Au target in the TNSA regime at PALS, reaching an energy of about 4.75 MeV at about 10 μm foil thickness, as described in recent literature [17]. Such effects of ion energy enhancement at the optimal foil thickness are strongly affected by the laser contrast and by the use of prepulses, but in the investigated experiment the contrast was very low and the prepulse was not used.

Discussion and conclusions

The laser plasma ion acceleration is becoming more and more a promising technique because nowadays with increasing the laser intensity up to values higher than 10^{20} W/cm² and decreasing the laser pulse duration to values of the order of 10 fs it is possible to accelerate protons up to energies of about 50 MeV and ions up to about 30 MeV/charge state. The main problems that remain to be solved are the ion energy spread, the multiple ion species present in the plasma emission, the low ion yield, the use of high laser repetition rates and the reproducibility of the laser shots and plasma properties.

The aspects regarding the plasma diagnostics and the measurements of ion energy distribution are of special interest for an on line monitoring, in order to inspect the plasma reproducibility and to evaluate with high precision the ionic emission properties. Using a correct diagnostic panel, for example, it is possible to have detailed information of the maximum ion energy, angular distribution, maximum charge states and spatial and temporal plasma dynamics. To this end the SiC detectors, resistant to high radiation dose and high temperatures, and Thomson parabola spectrometers, giving many plasma parameters information from single and fast laser shots, can be considered near indispensable for the plasma monitoring. However, other diagnostics are very useful, such as, for example, the interferometric imaging of the plasma, the use of track detectors and of fast CCD camera to observe the different photon emission [18].

The applications of the laser-generated plasmas technique are numerous and concern many different fields, depending on the kind of laser used, on the plasma parameters (temperature and density) and on the energy of radiated particles (photons, electrons and ions) emitted from the non-equilibrium plasma. The generation of any kind of ions, depending on the nature of the target, and the use of BPA regime with low laser intensity (~10^{10} W/cm²) using repetitive pulses, permits to realize laser ion sources with high efficiency and emission current. In this case, by using ion post-acceleration (1–100 kV) it is possible to generate ions to be injected into traditional accelerators – such as the ECLISSE experiment realized at INFN-LNS at Catania, in which Ta ions are injected into the Superconducting Cyclotron [19] – and it is possible to conduct ion implantation processes at high doses in order to modify the chemical and physical properties of many surface materials [20].

The TNSA regime is very interesting to accelerate light ions, such as protons, deuterons and carbons, at energies in the range 1–20 MeV, because it permits to induce many nuclear reactions in plasma. The deuterium–deuterium nuclear fusion processes, for example, can be obtained in laser-generated plasma at PALS by irradiating deuterated polyethylene targets and generating a number of nuclear events of the order of 10^8 per laser shot, producing 3.0 MeV protons and 2.5 MeV neutrons in a controllable manner [2].

The RPA regime, often associated to TNSA, permits to increase significantly the ion acceleration to energies above 10 MeV/charge state and proton acceleration above 50 MeV without the need to use traditional ion accelerators. Using special electro-magnetic ion selectors it is possible to obtain the ion selection on the basis of the atomic number, charge state and energy. For example it is possible to select protons from other ion species and to have monoenergetic component to be used in medicine. Such ions can be used for proton therapy, starting from 60 MeV, which is sufficient to cure superficial tumours, and reaching 100–200 MeV required to cure deep cancer tissues, depositing tens of Gray doses in a few laser shots. In this context the ELIMED project of INFN-LNS of Catania is giving interesting results [5].

Other interesting applications in the field of astrophysics, microelectronics, chemical industry and environment are also recommended by using high energetic ions produced by intense laser-generated plasma.

References

1. Gammino, S., Torrisi, L., Andò, L., Ciavola, G., Celona, L., Krasa, J., Laska, L., Pfeifer, M., Rohlena, K., Woryna, E., Wolowski, J., Parys,. P., & Shirkov, G. D. (2002). Production of low energy, high intensity metal ion beams by means of a laser ion source. *Rev. Sci. Instrum.*, *73*(2), 650–653.

2. Torrisi, L., Cavallaro, S., Cutroneo, M., Giuffrida, L., Krasa, J., Margarone, D., Velyhan, A., Kravarik, J., Ullschmied, J., Wolowski, J., Szydlowski, A., & Rosinski, M. (2012). Monoenergetic proton emission from nuclear reaction induced by high intensity laser-generated plasma. *Rev. Sci. Instrum.*, *83*, 02B111-4. DOI: 10.1063/1.3671741.

3. Maksimchuk, A., Gu, S., Flippo, K., Umstadter, D., & Bychenkov, V. Yu. (2000). Forward ion acceleration in thin films driven by a high-intensity laser. *Phys. Rev. Lett.*, *84*, 4108–4111. http://dx.doi.org/10.1103/PhysRevLett.84.4108.

4. Andò, L., Torrisi, L., Gammino, S., & *et al.* (2003). Laser ion source for multile Ta ion implantation. In Gammino-Mezzasalma-Neri-Torrisi (Eds.) Proceedings of PPLA2003, September 2003, Messina (pp. 142–148). Singapore: World Scientific Publ.

5. Cirrone, G. A. P., Carpinelli, M., Cuttone, G., Gammino, G., Bijan Jia, S., Korn, G., Maggiore, M., Manti, L., Margarone, D., Prokupek, J., Renis, M., Romano, F., Schillaci, F., Tomasello, B., Torrisi, L., Tramontana, A., & Velyhan, A. (2013). ELIMED, future hadron-therapy applications of laser-accelerated beams. *Nucl. Instrum. Methods Phys. Res. Sect. A-Accel. Spectrom. Dect. Assoc. Equip.*, *730*, 174–177. DOI: 10.1016/J.nima.2013.05.051.

6. Torrisi, L., Caridi, F., Giuffrida, L., Torrisi, A., Mondio, G., Serafino, T., Caltabiano, M., Castrizio, E. D., Paniz, E., & Salici, A. (2010). LAMQS analysis applied to ancient Egyptian bronze coins. *Nucl. Instrum. Methods Phys. Res. Sect. B-Beam Interact. Mater. Atoms*, *268*, 1657–1664. DOI: 10.1016/j.nimb.2010.03.015.

7. Eliezer, S. (2002). *The interaction of high-power lasers with plasmas*. Bristol: IOP.

8. Laska, L., Cavallaro, S., Jungwirth, K., Krasa, J., Krousky, E., Margarone, D., Mezzasalma, A., Pfeifer, M., Rohlena, K., Ryc, L., Skala, J., Torrisi, L., Ullschmied, J., Velyhan, A., & Verona-Rinati, G. (2009). Experimental studies of emission of highly charged Au-ions and of X-rays from the laser-produced plasma at high laser intensities. *Eur. Phys. J. D*, *54*, 487–492. http://dx.doi.org/10.1140/epjd/e2008-00226-8.

9. Badziak, J., Głowacz, S., Jabłoński, S., Parys, P., Wołowski, J., Hora, H., Krása, J., Láska, L., & Rohlena, K. (2004). Production of ultrahigh ion current densities at skin-layer subrelativistic laser–plasma interaction. *Plasma Phys. Contr. Fusion*, *46*(12B), 044, 83111-7. DOI: 10.1088/0741-3335/46/12B/044.

10. Robinson, A. P. L., Zepf, M., Kar, S., Evans, R. G., & Bellei, C. (2008). Radiation pressure acceleration of thin foils with circularly polarized laser pulses. *New J. Phys.*, *10*, 1367-1-13. DOI: 10.1088/1367-2630/10/1/013021.

11. Garcia, M. A. (2011). Surface plasmons in metallic nanoparticles: fundamentals and applications. *J. Phys. D-Appl. Phys.*, *44*, 283001(20pp.). DOI: 10.1088/0022-3727/44/28/283001.

12. Wen, L., Li, X., Zhao, Z., Bu, S., Zeng, X.S., Huang, J., & Wang, Y. (2012). Theoretical consideration of III–V nanowire/Si triple-junction solar cells. *Nanotechnology*, *23*(50), 505202–505211. DOI: 10.1088/0957-4484/23/50/505202.

13. Nanopartz™ Bare Gold Nanorodz. (2014). http://www.nanopartz.com/bare_gold_nanorods.asp.

14. Torrisi, L., Margarone, D., Laska, L., Krasa, J., Velyhan, A., Pfeifer, M., Ullschmied, J., & Ryc, L. (2008). Self-focusing effect in Au-target induced by high power pulsed laser at PALS. *Laser Part. Beams*, *26*, 379–387. http://dx.doi.org/10.1017/S0263034608000396.

15. Vector Field Software. (2014). http://www.vector-fields.co.uk/.

16. Thum-Jager, A., & Rohr, K. (1999). Angular emission distributions of neutrals and ions in laser ablated particle beams. *J. Phys. D-Appl. Phys.*, *32*, 2827–2832. DOI: 10.1088/0022-3727/32/21/318.

17. Torrisi, L., Cutroneo, M., Andò, L., & Ullschmied, J. (2013). Thomson parabola spectrometry for gold laser-generated plasmas. *J. Phys. Plasmas*, *20*, 023106-1-7. http://dx.doi.org/10.1063/1.4793454.

18. Láska, L., Badziak, J., Jungwirth, K., Kálal, M., Krása, J., Krouský, E., Kubeš, P., Margarone, D., Parys, P., Pfeifer, M., Rohlena, K., Rosinski, M., Ryc, L., Skála, J., Torrisi, L., Ullschmied, J., Velyhan, A., & Wolowski, J. (2010). Analysis of processes participating during intense iodine-laser-beam interactions with laser-produced plasmas. *Radiat. Eff. Defects Solids*, *165*(6/10), 463–471. DOI: 10.1080/10420151003718550.

19. Gammino, S., Torrisi, L., Consoli, F., Margarone, D., Celona, L., & Ciavola, G. (2008). Perspectives for the ECLISSE method with 3rd generation ECRIS. *Radiat. Eff. Defects Solids*, *163*(4/6), 277–286. DOI: 10.1080/10420150701777868.

20. Torrisi, L., Gammino, S., Mezzasalma, A. M., Badziak, J., Parys, P., Wolowski, J., Woryna, E., Krása, J., Láska, L., Pfeifer, M., Rohlena, K., & Boody, F. P. (2003). Implantation of ions produced by the use of high power iodine laser. *Appl. Surf. Sci.*, *217*, 319–331. DOI: 10.1016/S0169-4332(03)00551-8.